High-Fidelity Transport of Trapped-Ion Qubits through an X-Junction Trap Array

R. B. Blakestad, C. Ospelkaus, A. P. VanDevender, J. M. Amini, J. Britton, D. Leibfried, and D. J. Wineland

National Institute of Standards and Technology, 325 Broadway, Boulder, Colorado 80305, USA
(Received 8 February 2009; published 16 April 2009)

We report reliable transport of $^9\mathrm{Be}^+$ ions through an "X junction" in a 2D trap array that includes a separate loading and reservoir zone. During transport the ion's kinetic energy in its local well increases by only a few motional quanta and internal-state coherences are preserved. We also examine two sources of energy gain during transport: a particular radio-frequency noise heating mechanism and digital sampling noise. Such studies are important to achieve scaling in a trapped-ion quantum information processor.

Key requirements for efficient large-scale quantum information processing (QIP) include reliable transport of information throughout the processor and the ability to perform gates between arbitrary qubits. Trapped ions are a useful system for studying elements of QIP [1–3] and can potentially satisfy these requirements. The multiqubit gates that have been demonstrated couple ions through a shared mode of motion [1–3], similar to the proposal in [4]. This mode should be cooled to the ground state for maximum fidelity, which has exceeded 0.99 [5] in demonstrations. However, as the number of ions N grows, it becomes increasingly difficult to address the desired mode without coupling to other modes. To achieve scalability, the ions could be distributed over separate trap zones where N for each zone remains small [6–8]. Information could be shared between zones by moving the ions [6–8] or connecting them with photons [2,9,10]. In the proposal of [6,8], multidimensional arrays incorporating junctions would enable ions selected from arbitrary locations to be grouped together for multiqubit gates. Ion transport between zones must be accomplished with high success probability and minimal kinetic energy gain to not adversely affect the fidelity of subsequent multiqubit gates [1–3]. Sympathetic cooling can restore the motional modes for gate operations [6,8], but for large kinetic energy, this costs significant time, accompanied by decoherence, and possible ion reordering.

Previously, ions have been transported in a linear array [11–15] and separated for further processing without loss of qubit coherence [11,12] and with minimal energy gain. Transport through a two-dimensional "T junction" has been achieved with Cd^+ ions [13]. However, in that experiment, the success probability for round-trip transit was 0.98, and ions experienced considerable energy gain, estimated to be ~1 eV, which would necessitate a substantial delay for recooling before performing subsequent gates. In this Letter, we report transport of $^9\mathrm{Be}^+$ ions through a junction with greater than 0.9999 probability and less than 10^{-7} eV energy gain.

The trap (Fig. 1), constructed from two laser-machined alumina wafers with gold-coated electrodes [11], is derived from a linear rf Paul trap. It was held in vacuum at $<5 \times 10^{-9}$ Pa, while a 1.44 mT B field along $\hat{y} - \hat{z}$ (the Doppler cooling and detection laser beam direction) provided the ion internal-state quantization axis. Radial confinement (perpendicular to the channel axes) was provided by an rf ($V_0 \approx 200$ V, $\Omega_{\mathrm{rf}}/2\pi \approx 83$ MHz) pseudopotential with axial confinement due primarily to quasistatic control potentials [11]. Two main channels intersect at zone $\mathcal{C}$ (center), forming an "X junction." In addition to $\mathcal{C}$, zones $\mathcal{E}$ (experiment), $\mathcal{H}$ (horizontal), and $\mathcal{V}$ (vertical), located in other legs of the junction, comprise the four destinations for transport. The lower leg of the X junction provides symmetry about $\mathcal{C}$ but lacks the required electrodes to separately hold ions. Typically, the imaging optics and laser beams were positioned at $\mathcal{E}$, though $\mathcal{L}$, $\mathcal{H}$, and $\mathcal{V}$ allow similar access. Laser beam parameters were similar to those in [11,12].
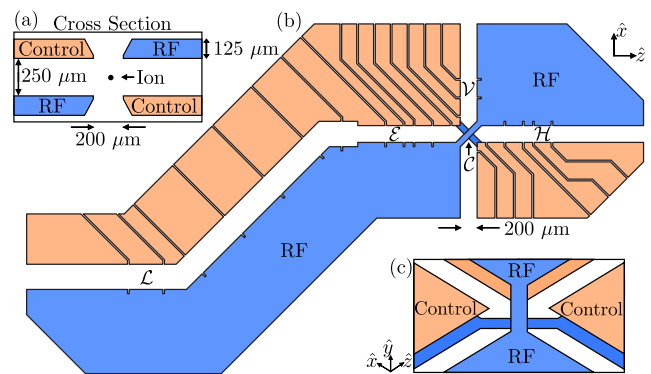
FIG. 1 (color online). (a) Cross-sectional view of the two layers of electrodes. (b) Top view of the electrode layout, with the rf electrodes indicated, and all other (control) electrodes held at rf ground. A nearly identical set of electrodes sits below these electrodes, with rf and control electrodes interchanged [11]. Forty-six control electrodes support 18 different trapping zones. The load zone ($\mathcal{L}$), the main experiment zone ($\mathcal{E}$), the vertical zone ($\mathcal{V}$), the horizontal zone ($\mathcal{H}$) and the center of the junction ($\mathcal{C}$) are labeled. (c) Schematic of the rf bridges from an oblique angle (not to scale).

Two diagonal bridges connect the rf electrodes across the junction [Fig. 1(c)]. These bridges induce pseudo-potential barriers (~ 0.35 eV) along the $\hat{x}$ and $\hat{z}$ channels, adjacent to the junction (Fig. 3), which must be overcome to transport ions through the junction. Narrow control electrodes (100 μm wide) near the junction accomplish this while using modest voltages ($|V| \leq 10$ V).

The time-varying potentials on the control electrodes were designed to produce a moving harmonic well (axial frequency ω_z) that adiabatically transported ions through the trap array and minimized energy gain in the motional mode. This appears to be a crucial difference from the experiments in [13] where, when the ions were transported across a pseudopotential barrier, they gained energy by falling from its apex. In our experiments, $\omega_z/2\pi$ increased from 3.6 MHz at $\mathcal{E}$, $\mathcal{H}$, and $\mathcal{V}$ to 5.7 MHz as the ion neared $\mathcal{C}$, where symmetry forces ω_z to be close to one of the two radial-mode frequencies. Radial frequencies ranged from 12 to 14 MHz except near $\mathcal{C}$, where one decreased to 5.7 MHz.

Ions are created in zone $\mathcal{L}$ by photoionizing neutral Be, which is delivered from a heated source. The electrodes of other zones are shielded from Be deposition by a mask (not shown). Zone $\mathcal{L}$ can be used as a reservoir for ions, but in the experiments here, ions are directly shuttled to $\mathcal{E}$ where they are laser cooled. Following transport to $\mathcal{C}$, $\mathcal{H}$, or $\mathcal{V}$, they were returned to $\mathcal{E}$, where the average harmonic occupation $\bar{n}$ was measured for the axial mode, yielding the motional-energy gain. We report three cases: transport to the junction's center and back ($\mathcal{E}$-$\mathcal{C}$-$\mathcal{E}$), transport through the junction horizontally ($\mathcal{E}$-$\mathcal{C}$-$\mathcal{H}$-$\mathcal{C}$-$\mathcal{E}$), and vertically ($\mathcal{E}$-$\mathcal{C}$-$\mathcal{V}$-$\mathcal{C}$-$\mathcal{E}$). By symmetry, all paths leading away from $\mathcal{C}$ are equivalent. Therefore, $\mathcal{E}$-$\mathcal{C}$-$\mathcal{E}$ transport and transporting through the junction once (i.e., $\mathcal{E}$-$\mathcal{C}$-$\mathcal{H}$) are analogous. In the adiabatic regime, for one ion we expect no additional energy gain due to turning the corner toward $\mathcal{V}$.

Energy gain after transport was determined using two independent methods (Table I). The Doppler recooling method [16,17] was sensitive to $\bar{n} \gtrsim 50$. For energy gain below 50 quanta/trip, this method required performing multiple transports before measurement. In the Rabi flopping method [11,18], which was sensitive for $\bar{n} \lesssim 100$, flopping curves on the "red" and "blue" sidebands or "carrier" of a stimulated-Raman-induced ground-state hyperfine transition were obtained. These curves were fit using calibrated Rabi rates for different Fock states $|n\rangle$ to extract $\bar{n}$. Fits assuming an arbitrary state, a thermal state, or a coherent state were made. Each assumption gave a slightly different result for $\bar{n}$ (range given in Table I) with no obvious preferred method. Nevertheless, the approximate agreement between recooling and flopping estimates lends confidence to the overall results.

The intrinsic heating rate for a stationary ion at $\mathcal{E}$ was measured to be 40 quanta/s, which negligibly affects the results. We expect that the dominant kinetic energy in-

TABLE I. Axial-motion energy gain for transport through the X junction, for one and two ^{9}Be$^+$ ions. Increase in the average motional state quantum number $\bar{n}$ was measured by two methods: "Doppler recooling" and "Rabi flopping" (see text). The energy gain is stated in units of quanta in a 3.6 MHz trapping well where $\bar{n} = 5$ quanta corresponds to 82 neV.

Transport		Energy gain (quanta/trip)	
		Recooling	Flopping
$\mathcal{E}$-$\mathcal{C}$-$\mathcal{E}$	1 ion	3.2 ± 1.8	5–12
$\mathcal{E}$-$\mathcal{C}$-$\mathcal{H}$-$\mathcal{C}$-$\mathcal{E}$	1 ion	7.9 ± 1.5	6–12
$\mathcal{E}$-$\mathcal{C}$-$\mathcal{V}$-$\mathcal{C}$-$\mathcal{E}$	1 ion	14.5 ± 2.0	7–14
$\mathcal{E}$-$\mathcal{C}$-$\mathcal{E}$	2 ions	5.4 ± 1.2	$\cdots$
$\mathcal{E}$-$\mathcal{C}$-$\mathcal{H}$-$\mathcal{C}$-$\mathcal{E}$	2 ions	16.6 ± 1.8	$\cdots$
$\mathcal{E}$-$\mathcal{C}$-$\mathcal{V}$-$\mathcal{C}$-$\mathcal{E}$	2 ions	53.0 ± 1.2	$\cdots$

crease will occur along the axis (the direction of transport), which is the direction employed in demonstrated qubit gates. This is supported by the approximate agreement of energy gains estimated using Rabi flopping (sensitive primarily to axial energy) and Doppler recooling (sensitive to both axial and transverse energy, but in the analysis, we attribute all heating to the axial mode). Transport between $\mathcal{C}$ and $\mathcal{E}$ or $\mathcal{H}$ (890 μm) took approximately 50 μs, with 20 μs to cross the pseudopotential barrier. Transport from $\mathcal{E}$ to $\mathcal{H}$ or $\mathcal{V}$ took approximately 100 μs.

To determine transport success, 10 000 $\mathcal{E}$-$\mathcal{C}$-$\mathcal{H}$-$\mathcal{C}$-$\mathcal{E}$ transports were performed while verifying that the ion always appeared in $\mathcal{E}$ as intended. Then 10 000 more transports were performed, now verifying that the ion always appeared in $\mathcal{H}$. With no observed failures in either set, we place a lower limit on the transport success probability of 0.9999. The same procedure was used to verify $\mathcal{E}$-$\mathcal{C}$-$\mathcal{V}$-$\mathcal{C}$-$\mathcal{E}$ transport with identical results. Ion lifetime, and thus transport success probability, would be ultimately limited by ion loss resulting from background-gas collisions [6]. With this in mind, we observed no increase in ion-loss rates over that for a stationary ion (~ 0.5/hr) during the transport experiments. By observing millions of successive round trips for the three types of transport, this suggests a success probability of greater than 0.999 995. Since transport comprised a small fraction of the total experiment duration, many of these losses likely occurred when the ion was not being transported.

Moving pairs of ions in the same trapping well would be useful for both sympathetic cooling and efficient ion manipulation [8]. We demonstrated such transport using pairs of ^{9}Be$^+$ ions and observed loss rates comparable to those for an ion pair held stationary. Additional heating mechanisms for multiple ions [6,19] may explain the higher transport energy gain observed for the pair (Table I). Additional energy was likely gained during rotation of the ion pair at $\mathcal{C}$ for the $\mathcal{E}$-$\mathcal{C}$-$\mathcal{V}$-$\mathcal{C}$-$\mathcal{E}$ transport. Single ^{24}Mg$^+$ ions have also been successfully transported.

For use in QIP, transport through a junction should preserve qubit coherence. To check this, we implemented a Ramsey experiment (Fig. 2) interleaved with junction transport. The ion was first prepared at $\mathcal{E}$ in the ground hyperfine state $|F = 2, m_F = -2\rangle$, which can be detected by fluorescence on a cycling transition. Coherent resonant Raman $\frac{\pi}{2}$ pulses transferred the ion into an equal superposition of the $|2, -2\rangle$ (fluorescing) and $|1, -1\rangle$ (nonfluorescing) state. This was followed by a free-precession period $T_1 = 280$ μs, a spin-echo π pulse (duration 1 μs), and a second free-precession period $T_2 = T_1$. Finally, the phase ϕ of a second $\frac{\pi}{2}$ pulse was varied and fluorescence was collected to generate a curve whose contrast is proportional to the ion's final coherence. The effect of transport on coherence was tested by inserting a single full $\mathcal{E}$-$\mathcal{C}$-$\mathcal{E}$ transport during both T_1 and T_2, during T_2 only, or not at all. The contrast when not transporting was only $85.0 \pm 0.5\%$ due to the length of the experiment. However, the contrast for one and two transports was $86.0 \pm 0.5\%$ and $85.6 \pm 0.5\%$, respectively, implying that transport does not affect coherence within the measurement errors. A difference in the B-field magnitude ($\frac{\Delta B}{B} \approx 0.4\%$) over the 890 nm path from $\mathcal{E}$ to $\mathcal{C}$, which results in a variable transition frequency, induced a phase shift when only one transport was inserted, but the spin-echo effectively canceled this phase when the transport was performed twice.

To obtain the results in Table I, careful attention was paid to sources of heating. Noise on the rf pseudopotential can cause ion heating [6,20,21], but this is negligible for an ion on the rf electric-field null. However, similar

(a)

(b)

FIG. 2 (color online). (a) Pulse sequence for the Ramsey experiment showing the two $\frac{\pi}{2}$ pulses with free-precession periods $T_1 = T_2$ and a spin-echo π pulse. (b) Fluorescence versus the final $\frac{\pi}{2}$ pulse phase ϕ for three cases where a single full $\mathcal{E}$-$\mathcal{C}$-$\mathcal{E}$ transport was inserted during both T_1 and T_2, during T_2 only, or not at all.

heating resurfaces when the ion is placed in a pseudo-potential gradient [6], which is typical for junction transport [22] and can be an issue for surface-electrode traps [23]. We examine the case of an axial pseudopotential gradient, as this caused heating along the pseudopotential barriers near $\mathcal{C}$.

Consider an rf trap drive with a voltage noise component at $\Omega_{\rm rf} + \omega$, where $\Omega_{\rm rf}$ is the drive frequency and $|\omega| \ll \Omega_{\rm rf}$. The trapping electric field will have the form

$$\vec{E}_{\rm rf}(x, y, z, t) = \vec{E}_0(x, y, z)[\cos\Omega_{\rm rf}t + \xi_N \cos(\Omega_{\rm rf} + \omega)t],$$

$$(1)$$

where $\xi_N \ll 1$ is the noise amplitude relative to $\vec{E}_0$, the ideal field. For $\xi_N = 0$, the above equation leads to the usual pseudopotential energy

$$\Phi_p = \frac{q^2}{2m\Omega_{\rm rf}^2}\langle \vec{E}_{\rm rf}^2(x, y, z, t)\rangle,$$

$$(2)$$

where m and q are the ion's mass and charge and the time average is performed over the period $2\pi/\Omega_{\rm rf}$. The addition of the noise term, which beats with the carrier, introduces a noise force on the ion at frequency ω. If we take the example of $\mathcal{E}$-$\mathcal{C}$ transport (restricting the ion to the $\hat{z}$ axis, where the field points along $\hat{z}$), $\vec{E}_0(x, y, z)$ simplifies to $E_0(z)\hat{z}$. This yields a noise force ($-\vec{\nabla}\Phi_p$) on the ion given by

$$\vec{F}_N \approx -\frac{q^2}{2m\Omega_{\rm rf}^2}\left(\frac{\partial}{\partial z}E_0^2(z)\right)\xi_N \cos(\omega t)\hat{z}.$$

$$(3)$$

Equation (3) can be used to relate broad-spectrum voltage noise, given by a voltage spectral density S_{V_N}, to force noise spectral density S_{F_N}, by use of $S_{V_N}/V_0^2 = S_{E_N}/E_0^2$, where V_0 is the peak rf potential applied to the trap and S_{E_N} is the noise spectral density of electric-field fluctuations $E_N = \xi_N E_0 \cos(\Omega_{\rm rf} + \omega)t$. For ω near the axial-mode frequency ω_z, S_{F_N} heats the mode according to the rate $\dot{n} = S_{F_N}(\omega_z)/4m\hbar\omega_z$ [21]. Therefore, the heating rate for noise applied around $\Omega_{\rm rf} + \omega_z$ is

$$\dot{n} = \frac{q^4}{16m^3\Omega_{\rm rf}^4\hbar\omega_z}\left[\frac{\partial}{\partial z}E_0^2(z)\right]^2\frac{S_{V_N}(\Omega_{\rm rf} + \omega_z)}{V_0^2}.$$

$$(4)$$

To test this, the ion was moved to a particular location along the axis between $\mathcal{E}$ and $\mathcal{C}$ and held there for a variable amount of time (≥ 1 ms) while we injected various amounts of band-limited white noise (flat to 1 dB over 150 kHz) centered at the lower sideband $\Omega_{\rm rf} - |\omega_z|$ onto the trap rf drive. The ion was returned to $\mathcal{E}$ and its temperature increase was measured by use of the recooling method. Figure 3 plots the ratio of measured heating rate to injected S_{V_N} and theoretical values of this ratio according to Eq. (4) based on simulations of trap potentials, for the ion held at several positions between $\mathcal{E}$ and $\mathcal{C}$. The deviation between the measured and predicted heating seems not
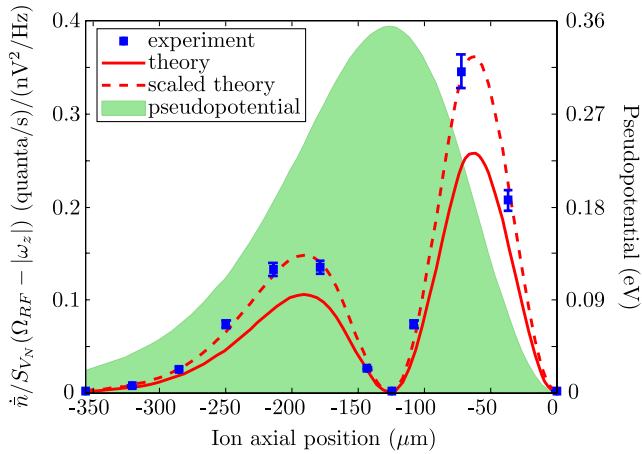
FIG. 3 (color online). The ratio of heating rate $\dot{n}$ to voltage noise spectral density $S_{V_N}(\Omega_{\rm rf} - |\omega_z|)$ for various locations along the trap axis ($\mathcal{C}$ is located at 0 μm). The theoretical prediction is shown both with and without a scaling parameter ($=1.4$). The simulated pseudopotential is overlaid in the background, in units of eV. Since heating is gradient dependent, we see very little heating at the peak of the pseudopotential barrier, despite it being the point of maximum (axial) rf electric field and ion micromotion. Nearly identical pseudopotential barriers occur on the other three legs of the junction.

unreasonable given the large number of experimental variables involved that are difficult to measure directly.

We limited this heating during transport through extensive rf filtering and by moving the ion over the barrier as fast as possible. From heating measurements without added noise, we estimate the ambient $S_{V_N}(\Omega_{\rm rf} \pm \omega_z)$ to be -177 dBc. For the transport durations used for the experiments in Table I, this S_{V_N} should impart ~ 0.1 to 0.5 quanta per pass over an rf barrier.

The other main source of energy gain was due to the digital-to-analog converters (DACs) that supply the waveforms. While transporting through a region far from the junction and using a fixed axial frequency (3.6 MHz), we observed energy gain when the DAC update rate (0.3–0.5 MHz) was commensurate with the motional frequency. When varying the update frequency, this energy gain exhibited a resonance at several submultiples of motional frequency with a bandwidth that decreased when the waveforms were stretched over more updates, consequently increasing the transport duration. This is as expected from coherent excitation. Use of an incommensurate update rate minimized this energy gain. However, minimizing the rf-noise heating required fast transport which broadened the resonances. This caused them to overlap, resulting in unavoidable energy gain. The effect was further compounded by the changing axial frequency during full junction transport and we experimented to find an update rate that minimized the total energy gain. Faster DACs and strong filtering of the potentials should alleviate this issue.

In summary, we have demonstrated reliable ion transport through a 2D trap junction with low motional-energy gain while maintaining internal-state qubit coherence. At these energies, sympathetic cooling could be employed for re-cooling in a reasonable period (for our current parameters, cooling from motional state $n = 5$ back to $n = 0$ would require 100 μs), while some quantum gates are robust against small energy gain [24–27] and may require only minimal recooling. Including recooling, the transport duration is comparable to other QIP processes for our system, and junction transport should not significantly slow QIP algorithms. Thus, this work demonstrates the viability of trap arrays incorporating junctions for use in large-scale QIP using trapped ions.

[1] R. Blatt and D. J. Wineland, Nature (London) **453**, 1008 (2008).
[2] C. Monroe and M. D. Lukin, Phys. World **21**, 32 (2008).
[3] H. Häffner, C. Roos, and R. Blatt, Phys. Rep. **469**, 155 (2008).
[4] J. I. Cirac and P. Zoller, Phys. Rev. Lett. **74**, 4091 (1995).
[5] J. Benhelm et al., Nature Phys. **4**, 463 (2008).
[6] D. J. Wineland et al., J. Res. Natl. Inst. Stand. Technol. **103**, 259 (1998).
[7] J. I. Cirac and P. Zoller, Nature (London) **404**, 579 (2000).
[8] D. Kielpinski, C. Monroe, and D. J. Wineland, Nature (London) **417**, 709 (2002).
[9] R. G. DeVoe, Phys. Rev. A **58**, 910 (1998).
[10] D. Moehring et al., J. Opt. Soc. Am. B **24**, 300 (2007).
[11] M. A. Rowe et al., Quantum Inf. Comput. **2**, 257 (2002).
[12] M. D. Barrett et al., Nature (London) **429**, 737 (2004).
[13] W. K. Hensinger et al., Appl. Phys. Lett. **88**, 034101 (2006).
[14] D. Stick et al., Nature Phys. **2**, 36 (2006).
[15] G. Huber et al., New J. Phys. **10**, 013004 (2008).
[16] R. J. Epstein et al., Phys. Rev. A **76**, 033411 (2007).
[17] J. H. Wesenberg et al., Phys. Rev. A **76**, 053416 (2007).
[18] D. M. Meekhof et al., Phys. Rev. Lett. **76**, 1796 (1996).
[19] H. Walther, Adv. At. Mol. Phys. **31**, 137 (1993).
[20] T. A. Savard, K. M. O'Hara, and J. E. Thomas, Phys. Rev. A **56**, R1095 (1997).
[21] Q. A. Turchette et al., Phys. Rev. A **61**, 063418 (2000).
[22] J. H. Wesenberg, Phys. Rev. A **79**, 013416 (2009).
[23] J. Chiaverini et al., Quantum Inf. Comput. **5**, 419 (2005).
[24] K. Mølmer and A. Sørensen, Phys. Rev. Lett. **82**, 1835 (1999).
[25] G. Milburn, S. Schneider, and D. James, Fortschr. Phys. **48**, 801 (2000).
[26] E. Solano, R. L. de Matos Filho, and N. Zagury, Phys. Rev. A **59**, R2539 (1999).
[27] C. Ospelkaus et al., Phys. Rev. Lett. **101**, 090502 (2008).